LagMemo: Language 3D Gaussian Splatting Memory for Multi-modal Open-vocabulary Multi-goal Visual Navigation

Haotian Zhou, Xiaole Wang, He Li, Fusheng Sun, Shengyu Guo, Guolei Qi, Jianghuan Xu, Huijing Zhao

Abstract-Navigating to a designated goal using visual information is a fundamental capability for intelligent robots. Most classical visual navigation methods are restricted to single-goal, single-modality, and closed set goal settings. To address the practical demands of multi-modal, open-vocabulary goal queries and multi-goal visual navigation, we propose LagMemo, a navigation system that leverages a language 3D Gaussian Splatting memory. During exploration, LagMemo constructs a unified 3D language memory. With incoming task goals, the system queries the memory, predicts candidate goal locations, and integrates a local perception-based verification mechanism to dynamically match and validate goals during navigation. For fair and rigorous evaluation, we curate GOAT-Core, a high-quality core split distilled from GOAT-Bench tailored to multi-modal open-vocabulary multi-goal visual navigation. Experimental results show that LagMemo's memory module enables effective multi-modal open-vocabulary goal localization, and that LagMemo outperforms state-ofthe-art methods in multi-goal visual navigation. Project page: https://weekgoodday.github.io/lagmemo

I. INTRODUCTION

In real-world applications such as home assistants and service robots, mobile agents are expected to understand user instructions, perceive environments, and navigate to target objects [1][2]. With the advancement of vision-language models [3][4], and inspired by the fact that humans primarily rely on vision to navigate, visual navigation has emerged as a prominent research area [1][5]. This task requires robots to rely primarily on visual sensors to reach target destinations in a safe and efficient manner.

Compared to the commonly studied single-goal, single-modality, closed set settings [6][7], real-world navigation is substantially more complex. Robots are often required to complete multiple tasks within the same environment, with goals specified in a multi-modal way, and these goals may involve categories not pre-defined in a close set. Therefore, this work focuses on multi-modal open-vocabulary multigoal visual navigation, as illustrated in Fig. 1. This formulation poses significant challenges for visual navigation systems.

To address this, GOAT-Bench [8] provides a dataset and baseline algorithms based on the Habitat simulator [9]. However, existing methods remain limited. End-to-end approaches like RL GOAT [8] encode the environment implicitly through hidden states, leading to poor generalization. Modular approaches like Modular GOAT [10] rely on 2D

Haotian Zhou and Huijing Zhao are with the Key Laboratory of Machine Perceptions (MOE), School of Intelligence Science and Technology, Peking University, Beijing, 100084, China (e-mail: zhoutiantian19@pku.edu.cn, zhaohj@pku.edu.cn).

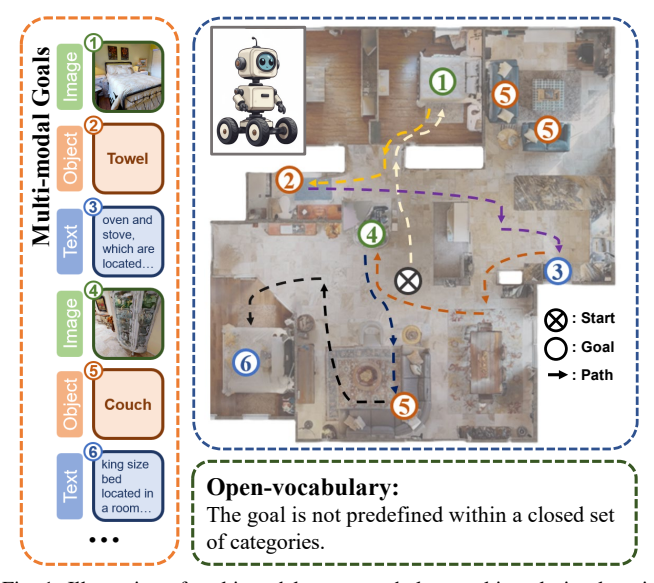


Fig. 1: Illustration of multi-modal open-vocabulary multi-goal visual navigation task. Multi-modal: the goal can be specified in the forms of an object category, an image or a text description; Open-vocabulary: the agent is not limited to navigating to a predefined closed set of categories; Multi-goal: the agent is required to find multiple goals within the same environment.

semantic maps and are restricted to a predefined set of categories, making them unsuitable for open-vocabulary setting.

In this work, we introduce LagMemo, which, to the best of our knowledge, is the first to use 3DGS with language features in visual navigation. LagMemo actively builds a 3DGS-based representation during exploration, storing both geometric and language information of the environment. During navigation, it supports multi-modal queries to identify candidate waypoints, improving navigation efficiency.

Our main contributions are summarized as follows:

- We propose LagMemo, a visual navigation system that is the first to use 3D Gaussian Splatting with codebookbased language feature embedding as a memory module. A keyframe retrieval mechanism is incorporated to adapt to sparse observations during navigation, enabling effective localization of multi-modal, open-vocabulary goals within a single exploration.
- We design a goal verification mechanism that bridges memory and perception. This mechanism operates through a cyclic process of memory query and perception-based validation, effectively leveraging the constructed memory to improve navigation success rate.
- Based on GOAT-Bench, we curate a high-quality household environment split named GOAT-Core, which can be used to evaluate both goal localization and multi-

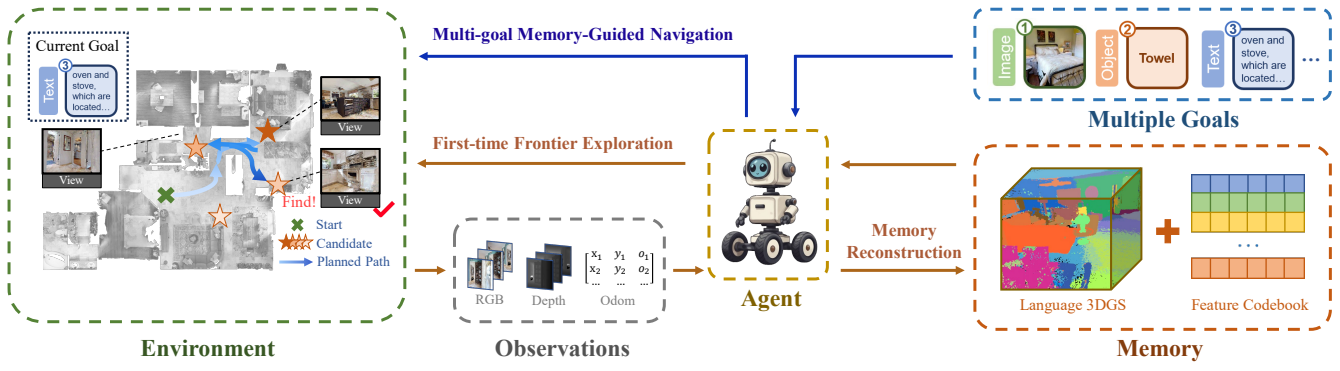


Fig. 2: LagMemo Overview. The agent first performs frontier-based exploration to collect observations from the environment, upon which it reconstructs a language 3DGS memory and a feature codebook. As multi-modal open-vocabulary goals input, the agent queries the memory to generate candidate localization regions and uses real-time perception to verify targets, thereby accomplishing multi-goal visual navigation.

modal multi-goal visual navigation tasks.

 Extensive quantitative experiments and case studies demonstrate that LagMemo achieves superior performance in both goal localization and multi-modal multigoal visual navigation tasks, surpassing current state-ofthe-art methods.

II. RELATED WORKS

A. Visual Navigation

In terms of methodology, early visual navigation approaches can be broadly categorized into modular [7][11] and end-to-end [12][13] frameworks. Several studies [14] have demonstrated that modular methods exhibit stronger robustness when transferred to real-world environments. Recent advances in large language models and vision-language models have led to a surge in zero-shot navigation methods [15][16][17][18]. These methods avoid task-specific retraining by leveraging commonsense knowledge embedded in pretrained foundation models [16][17][18]. In terms of goal modality, visual navigation tasks are commonly classified into ObjectGoal [19], ImageGoal [20], and TextGoal [21]. A key challenge in these settings is whether the target is limited to a closed set of categories. For example, SemExp [6] uses C channels in 2D semantic map to record the location of C predefined goal categories. Recent works [16][22] exploit CLIP or BLIP-2 to enable open-vocabulary identification and localization for novel goals. This paper focuses on multimodal open-vocabulary multi-goal visual navigation, a task formalized as lifelong visual navigation in GOAT [8][10], which is more aligned with practical applications.

B. Memory in Visual Navigation

In embodied visual navigation, effective memory of the environment is a critical factor for this long-horizon task. Some end-to-end approaches [12][23] employ RNN-based architectures such as LSTMs or GRUs to encode implicit memory. In contrast, modular methods typically adopt explicit map representations to store and utilize environmental information. A common paradigm is to use 2D semantic grid maps [6][7][16][24], which discretize the environment into spatial grids, assigning each grid a semantic label or high-dimensional embedding. Some works [25][26] construct scene graphs to model spatial relationships between objects

and rooms, facilitating long-term planning through graph-based reasoning. Recently, GaussNav [27] introduced 3D Gaussian Splatting (3DGS) as a memory representation, leveraging its fine-grained geometric rendering capabilities to distinguish object instances. It uses a closed category set and is primarily designed for instance image-goal navigation. In contrast, our work proposes a language 3DGS memory module that stores language features of objects, enabling multi-modal open-vocabulary querying.

C. 3D Gaussian Splatting with Language Embedding

3D Gaussian Splatting (3DGS) [28] is a 3D scene reconstruction method, which has attracted significant attention due to its high-quality and real-time rendering capabilities [29]. Several studies have explored online geometric modeling based on 3DGS [30][31]. As many embodied tasks require not only geometric representations but also semantic guidance, recent works [32][33][34][35] have attempted to incorporate language features extracted by 2D visionlanguage models into 3DGS model. For example, LangSplat [32] compresses high-dimensional CLIP features into lowdimensional Gaussian features. Most methods [32][33][34] optimize semantic features only in the rendered 2D view, their performance degrades when directly querying semantic features on 3D Gaussians. OpenGaussian [35] addresses this by proposing a feature discretization mechanism that aligns low-dimensional Gaussian features with high-dimensional 2D instance embeddings.

III. METHODOLOGY

A. Task and System Overview

We address the multi-modal, open-vocabulary, multi-goal visual navigation task in a multi-room indoor household environment. In this task setting, every episode comprises a sequence of subtasks, where the goal of the k^{th} subtask is denoted as g^k . At the beginning of each episode, the agent is randomly initialized. Every timestep t, the agent receives observations including an RGB image I_t^k , a depth image D_t^k , and odometry $p_t^k = (x_t^k, y_t^k, o_t^k)$, and outputs an action A_t^k . Only when current subtask is finished, will the next subtask goal g^{k+1} input. A subtask is deemed success when the agent executes STOP within a certain distance threshold from the target, and does not exceed maximum step limit.

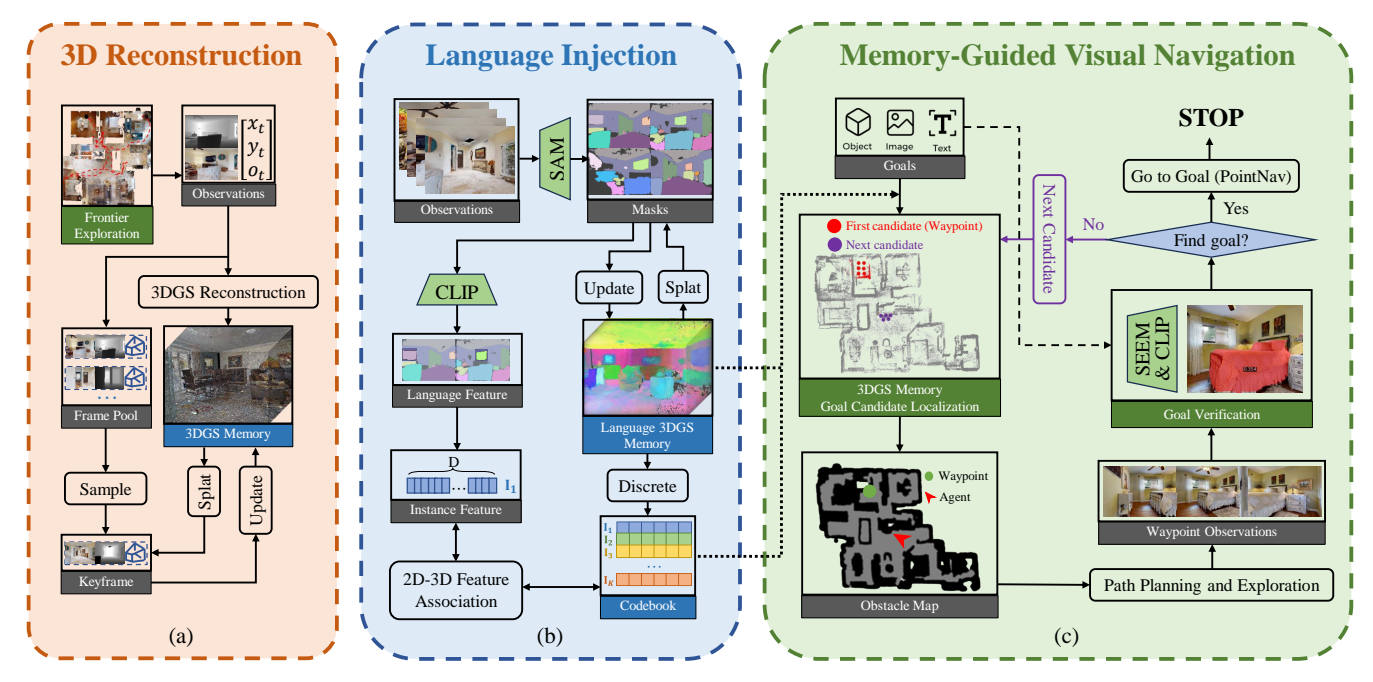


Fig. 3: Language 3DGS Memory Reconstruction and Memory-Guided Visual Navigation Pipeline. (a) 3D Reconstruction. During frontier exploration, the agent collects RGB, depth, and odometry to reconstruct 3DGS memory. A keyframe retrieval mechanism is employed to mitigate the forgetting and surface holes caused by sparse navigation views. (b) Language Injection. For image observations, we leverage SAM and CLIP to extract 2D semantic features. Via 2D-3D association, these features are assigned to Gaussians and discretized into a codebook. (c) Memory-Guided Visual Navigation. During execution, multi-modal open-vocabulary goals query the memory to propose candidate locations (waypoints). Using the obstacle map for path planning, the agent verifies the target to decide success or move to the next candidate.

The navigation goals are specified in one of three modalities: a category, an image, or a text description. Crucially, the task is open-vocabulary: the agent is not limited to navigating to objects from a predefined closed set of categories.

As illustrated in Fig.2, we propose LagMemo. The agent first conducts frontier-based exploration to proactively explore the environment. During this phase, a language 3D Gaussian Splatting (3DGS) memory is constructed (Sec.III-B). For subsequent subtasks, given a multi-modal goal, the agent queries the language 3DGS memory, and then navigates to the relevant object instances and verifies whether the observed objects match the goal (Sec.III-C).

B. Language 3DGS Memory Reconstruction

Frontier Exploration. The agent first performs frontier-based exploration [36] to traverse the environment. During this phase, the agent collects a stream of observations, including RGB, depth, and pose information, which are used for Gaussian-based geometry reconstruction. After exploration, a global optimization over the full frame sequence incorporates language features into the memory.

Geometry Reconstruction. This stage mainly follows [31], where 3D Gaussians are parameterized by spatial position $\mu \in \mathbb{R}^3$, color $c \in \mathbb{R}^3$, radius r, and opacity o. As illustrated in Fig. 3 (a), given incoming RGB-D frames and camera poses, new Gaussians are inserted in under-covered regions, and all parameters are optimized by the classical geometry loss that supervises both color and depth rendering:

$$\mathcal{L}_{geo} = (1 - \lambda)\mathcal{L}_1(\mathbf{C}) + \lambda\mathcal{L}_{SSIM}(\mathbf{C}) + \mu\mathcal{L}_1(D)$$
 (1)

In large-scale, multi-room navigation environments with limited inter-frame overlap, geometric reconstruction often suffers from forgetting and surface holes. To mitigate this, we introduce a keyframe retrieval mechanism. A frame pool stores all historical frames, which are periodically rendered and evaluated by PSNR against ground-truth. At each timestep, a two-stage optimization is performed: the current frame is optimized for p_1 iterations to ensure accurate reconstruction of new observations, followed by p_2 iterations on sampled historical frames. The sampling probability of a frame is inversely related to its PSNR, thus frames with lower fidelity are more likely to be revisited.

Language Injection. Following [35], as illustrated in Fig. 3 (b), we incorporate language information by optimizing the feature $f \in \mathbb{R}^d$ of each Gaussian and discretizing it into a codebook \mathcal{C} which is associated high-dimensional 2D instance features $f_{2d} \in \mathbb{R}^D$ extracted from image observations.

Concretely, instance masks are first obtained by SAM [37], and feature splatting is applied to render per-pixel semantic features. Mask-level features are aggregated and optimized with a feature loss that encourages intra-instance consistency and inter-instance separability. This ensures that Gaussians belonging to the same object share similar embeddings, while different objects remain distinguishable.

To achieve stable retrieval and cross-view instance alignment, Gaussian features are further discretized via a two-level codebook quantization. A coarse partition jointly considers 3D positions and language features, while a fine partition refines categories based solely on language features. Then we conduct a 2D-3D feature association between 2D

TABLE I: Data Comparison between GOAT-Core and GOAT-Bench of 4 Representative Rooms.

	Avg. Subtasks per Episode	Avg. Unique Categories per Episode	Avg. Inter-Subtask Distance (m)	Total Episodes	Total Subtasks 480	
GOAT-Core (Ours)	20	13.37	6.89	24		
GOAT-Bench (Original)	7.88	4.82	5.18	40	315	

instance-level features from multiple image views and the discretized 3D Gaussian language features. Specifically, for each instance category, we render all Gaussians assigned to that category and evaluate their spatial and semantic consistency with the 2D instance masks. The instance feature is then assigned to the discrete language category of the Gaussians with the highest similarity score.

This process produces a language codebook $\mathcal C$ where each entry corresponds to a cluster of 3D Gaussians enriched with CLIP features. During navigation, a multi-modal query (e.g., text or image) can be projected into the CLIP space and matched against $\mathcal C$ to retrieve candidate instances, enabling language-conditioned 3D memory.

C. Memory-Guided Visual Navigation

As illustrated in Fig. 3 (c), the proposed memory-guided navigation framework integrates goal localization, waypoint planning, goal verification, and final goalpoint navigation into a unified pipeline.

Goal Localization via Memory Query. The input goal, provided as either text or an image, is encoded into an embedding vector through the corresponding CLIP encoder. Cosine similarity is then computed against features of all entries stored in the codebook to identify candidate instance. The codebook records the indices of all Gaussians associated with the selected instance. Since navigation essentially requires guiding the agent towards the spatial location of the target instance, we compute the geometric centroid of all Gaussians linked to the instance and project it onto the 2D obstacle map. The resulting projection serves as the candidate position (waypoint) for navigation.

Waypoint Navigation. After calculating the corresponding goal position on the obstacle map, the position is dilated and intersected with the traversable region to define a feasible waypoint. A collision-free path from the agent's current position to the waypoint is then planned using the classical Fast Marching Method (FMM) [38].

Goal Verification and Matching. Upon reaching a waypoint, the agent first performs a panoramic scan for goal verification. For text and object goals, we incorporate SEEM [39] model for open-vocabulary instance segmentation, generating pixel-level masks for secondary validation. A waypoint is deemed to contain the target object if either the CLIP similarity or the mask confidence exceeds the corresponding thresholds. For image goals, LightGlue [40] feature matching is employed. If the goal is found, the system transitions into the Goalpoint Navigation stage. Otherwise, the waypoint is marked as invalid, and the memory is re-queried to obtain the next candidate instance. This iterative cycle of waypoint generation, navigation, and goal verification is repeated until the goal is found or the maximum step limit is reached.

Goalpoint Navigation. Once the verification mechanism confirms that the target object is visible in the current view, the problem reduces to determining the precise stopping position. Using the pixel-level masks provided by SEEM in combination with depth information, points on the target object are projected onto the obstacle map to define the final goalpoint. The agent then reuses the FMM algorithm to navigate and executes STOP to complete the subtask.

IV. BENCHMARK

The GOAT-Bench [8] dataset, built on Habitat, has been the primary benchmark for evaluating multi-modal, open-vocabulary, multi-goal visual navigation. Despite its diverse scenes, several limitations hinder its ability to reasonably assess navigation capabilities. First, the evaluation of long-term memory and planning is insufficient: each episode contains only about 8 subtasks on average, with high goal repetition and relatively short inter-goal distances. Second, annotation quality issues are present: some text descriptions are inaccurate, object categories are semantically ambiguous, and certain scenes include missing meshes or cross-floor tasks. These factors often cause agents to fail for reasons unrelated to algorithms, thereby obscuring fair comparison of navigation performance.

Instead of reporting on the entire GOAT-Bench validation split, which is broad but contains quality issues, we reorganize the benchmark by sampling a quality-controlled core subset GOAT-Core. As illustrated in Tab. I, we increase the number of subtasks per episode to 20 (compared to 7.88 in the original set) and enhance task diversity. The average distance between subtasks is also extended, imposing greater demands on memory and long-horizon planning. Although the number of episodes is reduced, we keep the aggregate number of subtasks non-decreasing. To ensure label reliability, we manually correct inaccurate or ambiguous text descriptions and prioritize objects with clear semantics. We further restrict all subtasks to occur on a single floor and

TABLE II: Goal Localization Results

Scene Method		Average	Object	Image	Text	
4ok	LagMemo VLMaps	86.7 % 63.3%	95.2 % 75.5%	73.0% 41.8%	88.6% 70.8%	
5cd	LagMemo VLMaps	65.0% 48.3%	80.2 % 62.1%	63.1% 39.4%	49.6% 42.7%	
Nfv	LagMemo VLMaps	66.7% 68.3%	85.5 % 80.0%	49.6% 46.8%	61.1% 73.6 %	
Tee	LagMemo VLMaps	65.0% 55.0%	92.6 % 61.3%	39.8% 45.1%	68.1% 56.9%	
Total	LagMemo VLMaps	70.8% 58.8%	88.4 % 69.7%	56.4% 43.3%	66.8% 61.0%	

TABLE III: Multi-modal Multi-goal Visual Navigation Results.

Method	Open-Vocabulary	Scene	Scene1-5cd		Scene2-4ok		Scene3-Nfv		Scene4-Tee		Total	
		SR	SPL	SR	SPL	SR	SPL	SR	SPL	SR	SPL	
GOAT - GT Sem*	×	70.0%	58.0%	88.3%	68.7%	63.3%	49.5%	78.3%	64.6%	75.0%	60.2%	
Modular GOAT [10]	×	28.3%	21.1%	45.0%	35.8%	38.3%	29.0%	41.7%	33.2%	38.3%	29.7%	
GOAT - Full Exp*	×	20.0%	16.7%	43.3%	36.3%	41.7%	30.0%	40.0%	30.8%	36.3%	28.5%	
RL GOAT [8]	✓	5.0%	3.5%	5.0%	1.7%	20.0%	11.3%	15.0%	9.0%	11.3%	6.2%	
CoWs* [15]	✓	26.7%	14.1%	63.3%	39.4%	41.7%	30.1%	51.7%	30.7%	45.8%	28.6%	
LagMemo (Ours)	✓	50.0%	31.0%	66.7%	38.2%	43.3%	26.1%	65.0%	45.8%	56.3%	35.3%	

select four reviewer-recommended high-quality multi-room scenes (5cd, 4ok, Nfv, Tee), each averaging 7.25 rooms, avoiding mesh defects or cross-floor navigation issues.

In total, GOAT-Core contains 480 multi-modal subtasks, covering 163 images, 158 objects, and 159 text goals. As in GOAT-Bench, the validation split includes both "unseen" and "seen-synonyms" categories relative to the training set, thereby supporting open-vocabulary evaluation. The dataset also explicitly emphasizes the multi-goal setting, with longer episodes and greater goal diversity compared to the original benchmark.

Beyond multi-goal visual navigation, GOAT-Core also enables the evaluation of goal localization tasks. For each of the four multi-room scenes (average area 218.63 m^2), we conduct full-house exploration via frontier exploration, collecting RGB, depth, and odometry data. The curated 480 multi-modal goal queries with ground-truth positions can thus be used to evaluate the accuracy of goal localization after mapping (Sec. V-A).

For navigation experiments, we use the HelloRobot Stretch model as the agent. The robot has a height of 1.41 m and a base radius of 17 cm. It is equipped with an RGB camera with a resolution of 640×480 , a horizontal field of view (HFOV) of 42° , mounted at a height of 1.31 m. The robot's depth perception range is $0.5 \sim 5.0$ m. Its action space consists of: MOVE_FORWARD (0.25 m), TURN_LEFT/RIGHT (30°), LOOK_UP/DOWN (30°), and STOP. A subtask is considered successful if the agent executes the STOP action within a 200-step limit and its final position is less than 1 m from the target object instance.

V. EXPERIMENTS

A. Goal Localization

Settings. 1) **Task:** The goal localization task requires mapping an open-vocabulary query to the memory constructed after frontier exploration and estimating the corresponding object's location, evaluated on the GOAT-Core.

2) **Baseline:** We use **VLMaps** [22] as baseline, which

TABLE IV: Memory Reconstruction Ablation Study.

Keyframe	Codebook	PSNR	Average	Object	Image	Text
×	✓	21.15	66.3%	77.5%	57.5%	63.4%
\checkmark	×	27.20	34.6%	41.6%	21.0%	37.1%
\checkmark	✓	27.20	70.8%	88.4%	56.4%	66.8%

constructs a visual-language map by projecting dense VLM features onto a 2D grid with depth and pose. 3) Metrics: Localization accuracy is measured by the Euclidean distance between predicted and ground-truth positions, with success defined as any of the top-5 predictions falling within a 1.5 m radius of the target. 4) Hyperparameters: Geometry optimization runs $p_1 = 30$ iterations per step for new viewpoints and $p_2 = 60$ iterations for keyframe viewpoints. Feature dimension d of Gaussians is 6. The two-level codebook uses coarse $k_1 = 32$ clusters and fine $k_2 = 5$ clusters per coarse cluster (total 160 entries).

Results. In goal localization, as illustrated in Tab. II, Lag-Memo achieves an overall 70.8% success rate, significantly outperforming VLMaps (58.8%) and across object (88.4% vs 69.7%), image (56.4% vs 43.3%), and text (66.8% vs 61.0%) modalities. This improvement arises from LagMemo's usage of language 3DGS, which preserves detailed 3D spatial context for accurate localization, whereas VLMaps compresses features into a 2D grid, losing critical geometric information. These results highlight the effectiveness of explicit 3D semantic memory for precise goal localization in complex environments.

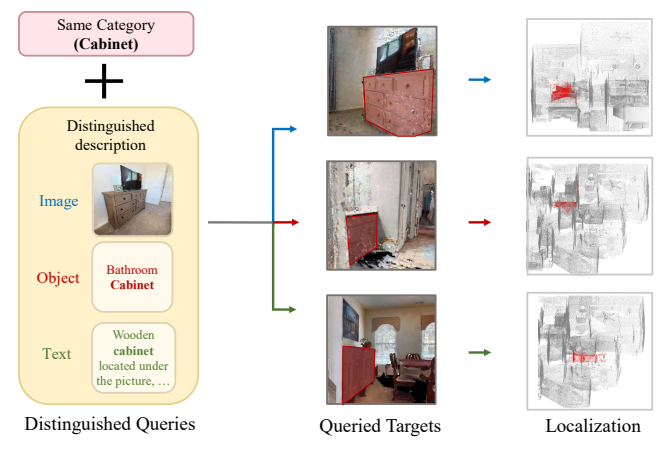


Fig. 4: Distinguished Queries Retrieving Different Instances of the Same Category in Language 3DGS Memory. For the same "cabinet" category, with distinguished queries, the language memory can retrieve the intended target. The middle column shows a geometric rendering containing queried target, and the right column presents the 3D localization of that instance.

We also provide visualizations to demonstrate our method's precise and context-aware goal localization. As shown in Fig. 4, our system is capable of fine-grained discrimination among multiple instances of the same category.

TABLE V: Goal Verification Ablation Study.

Goal Verification	Image Match	Text Match	Average		Object		Image		Text	
			SR(†)	SPL(↑)	SR(↑)	SPL(↑)	SR(↑)	SPL(↑)	SR(↑)	SPL(†)
×	-	-	41.3%	30.4%	45.1%	28.7%	32.9%	27.7%	45.1%	34.6%
√	CLIP	CLIP	46.7%	30.3%	52.4%	22.7%	43.4%	35.1%	43.9%	33.4%
√	LightGlue	SEEM + CLIP	56.3%	35.3%	68.3%	36.2%	46.1%	27.2%	53.7%	41.8%

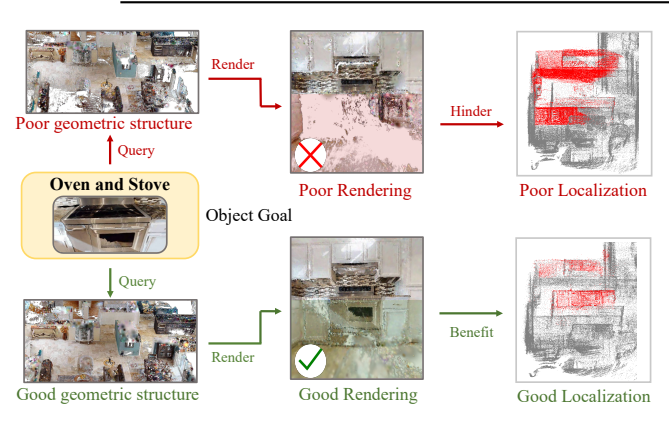


Fig. 5: Impact of Geometric Quality on Localization Precision. (Top) A poorly reconstructed geometric structure leads to diffuse and inaccurate localization. (Bottom) A high-quality geometry provides a strong anchor for semantic features, enabling precise localization.

Fig. 5 illustrates that a well-reconstructed geometric structure is crucial for accurate localization, whereas poor geometry leads to diffuse and inaccurate results.

B. Visual Navigation

1) Task: The visual navigation task requires Settings. the agent to reach multiple goal objects (Sec. III-A). At every timestep, given visual observations as input, the agent outputs an action to interact with the environment. The task is evaluated on the GOAT-Core (Sec. IV), a high-quality, statistically meaningful, and relatively fair evaluation split. As LagMemo involves no task-specific training, there is no test-set leakage. All baselines are also evaluated on the same GOAT-Core split for fair comparison. 2) Baselines: We compare LagMemo against five baselines. RL GOAT [8]: the official reinforcement learning baseline of GOAT-Bench, which encodes multi-modal goals with CLIP and directly maps observations and goals to actions. Modular GOAT [10]: a closed set modular approach that builds a 2D object map from detection results for navigation. **GOAT** - GT Sem*: a variant of Modular GOAT using groundtruth semantic segmentation results from simulator, serving as an upper bound for reference. GOAT - Full Exp*: a Modular GOAT variant with first pre-exploration, aligned with LagMemo for fairer comparison. CoWs*: adapted from the CoWs [15] method that combines frontier exploration with CLIP-based detection, extended here with multi-modal inputs. For closed set methods, we provide the list of target categories in advance to ensure feasibility, as these methods cannot operate without predefined categories. 3) Metrics: Performance is assessed using two common metrics: SR (Success Rate), which measures the proportion of successful

subtasks, and SPL (Success weighted by Path Length), which evaluates efficiency by comparing the trajectory length of successful episodes to the optimal path. 4) Hyperparam-The goal verification module is triggered when the agent is within 1.2 m of the candidate waypoint. For object/text goals, goal verification passes if either threshold is met: SEEM score $\tau_{SEEM} \geq 1.1$ or Mobile-CLIP cosine similarity $\tau_{CLIP} \geq 0.23$. For image goals, LightGlue declares target presence if the inlier match ratio $r_{match} \geq 5\%$. From a scene-wise perspective, Table III shows that LagMemo consistently achieves the highest success rate across all environments. On average, LagMemo outperforms the second-best baseline CoWs* by 10% in SR, and surpasses Modular GOAT by 18%. From a modality perspective, Fig. 6 shows that LagMemo demonstrates particularly strong advantages in text-based navigation tasks, outperforming all other baselines by a clear margin. Under the same preexploration setting, LagMemo achieves an improvement of SR +20% and SPL +6% compared with Modular GOAT, confirming the benefit of richer 3D semantic representations. Overall, LagMemo achieves the best SPL (35.3%). While slightly lower SPL is observed in 40k and Nfv, this is mainly due to the strict goal verification mechanism, which sacrifices some efficiency but ensures substantially higher success rates.

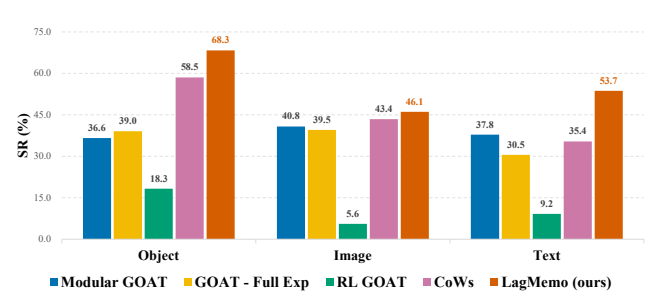


Fig. 6: Navigation Performance across 3 Modalities.

In addition to the quantitative results, we provide case studies to illustrate our method's effectiveness. Fig. 7 visualizes a step-by-step navigation task for an image goal ("oven and stove"), which demonstrates an effective interplay between long-term memory guidance and goal verification mechanism. Fig. 8 highlights LagMemo's robustness across object, image, and text goals, where the baseline fails, which underscores the advantage of our 3DGS memory.

C. Ablation Study

(1) Ablation on Memory Reconstruction. We conduct an ablation study to validate the keyframe retrieval mechanism and the discrete language codebook in our 3DGS memory

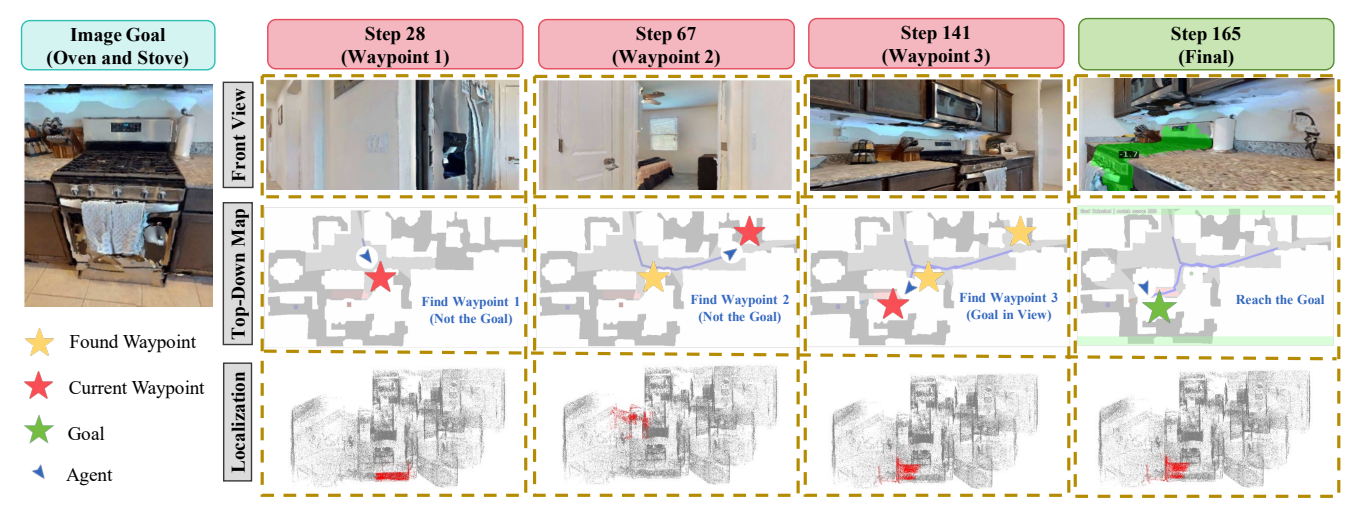


Fig. 7: Step-by-step Visualization of Memory-Guided Navigation to an Image Goal. Columns show key steps (28, 67, 141, 165), rows show the front view, the top-down map, and the 3D localization results (red). In this case, the agent reaches waypoint-1/2/3 (yellow star; current waypoint in red). After checking the first two, it arrives at the third where the goal verification module identifies the goal. Then the agent proceeds to the final goal (green star) and the subtask successfully terminates at step 165.



Fig. 8: Qualitative Comparison of LagMemo against the Modular GOAT (Baseline). We present three cases with different goal modality: object (left), image (middle), text (right). LagMemo retrieves the intended instance from the language 3DGS memory, plans on the top-down map, and verifies success. Modular GOAT (baseline) either selects a wrong instance or fails to find any instance, reflecting the limits of its 2D semantic memory to form a complete and correct representation of the scene.

module. The results are shown in Tab. IV. Removing the keyframe mechanism degrades reconstruction quality (PSNR drops from 27.20 to 21.15) and lowers localization accuracy from 70.8% to 66.3%, confirming that accurate geometry is foundational for goal localization. In language injection, it's critical to use language codebook to associate high-dimensional features with 3D Gaussians. To ablate the effect of the codebook, we adopted an approach referred to LangSplat [32]: using an autoencoder trained on 2D images to encode low-dimensional Gaussian features and and decoding the feature when querying. Despite maintaining the same geometry reconstruction method, the average localization accuracy drops to 34.6%. This highlights that features trained on 2D images, without the explicit 3D spatial clustering and semantic association are insufficient for building a consistent

and queryable memory for multi-room object localization.

(2) Ablation on Goal Verification Mechanism. We perform an ablation study to analyze the impact of our goal verification module, with results presented in Table V. The baseline approach, which stops at the first reached region without any verification, achieves an average SR of 41.3%. Introducing a generic CLIP-based similarity scoring yields a modest improvement, increasing the SR to 46.7%. Our final approach employs the modality-specific strategy (see Sec. III-C), achieving the highest performance with an SR of 56.3% and an SPL of 35.3%. This demonstrates that a sophisticated, modality-specific verification mechanism is crucial for confirming the final stopping point, significantly enhancing both success rate and navigation efficiency.

VI. CONCLUSIONS

We present LagMemo, a navigation system that integrates language 3D Gaussian Splatting to address the practical demands of visual navigation with multi-modal and open-vocabulary goal inputs as well as multi-goal tasks. By encoding language features into memory through single exploration and employing perception-based goal verification mechanism, LagMemo enables efficient goal localization and reliable navigation. Extensive experiments and case studies demonstrate consistent improvements over state-of-the-art methods in both goal localization and multi-goal navigation.

Despite the encouraging results in integrating semantic 3D memory with visual navigation, several directions remain open. (1) Memory-aware Exploration. LagMemo's goal localization capability hinges on geometric fidelity, insufficient view coverage leaves blind spots in memory. Future work includes developing memory-aware active exploration that leverages geometric and semantic uncertainty to select informative views and close gaps. (2) Incremental Semantics. Real environments are dynamic (rearrangements, additions, removals), whereas our memory is largely static and fixed-capacity. We will build incremental, lifelong language 3DGS

with online codebook growth and merging. (3) Pruning and Compression. Full-scene 3D representations are memory-intensive. A promising direction is to pursue hierarchical or multi-resolution Gaussians, uncertainty-aware pruning, and feature compression.

REFERENCES

- M. Deitke, D. Batra, Y. Bisk, T. Campari, A. X. Chang, D. S. Chaplot, C. Chen, C. P. D'Arpino, K. Ehsani, A. Farhadi et al., "Retrospectives on the embodied ai workshop," arXiv preprint arXiv:2210.06849, 2022.
- [2] J. Sun, J. Wu, Z. Ji, and Y.-K. Lai, "A survey of object goal navigation," *IEEE Transactions on Automation Science and Engineering*, 2024.
- [3] A. Radford, J. W. Kim, C. Hallacy, A. Ramesh, G. Goh, S. Agarwal, G. Sastry, A. Askell, P. Mishkin, J. Clark et al., "Learning transferable visual models from natural language supervision," in *International* conference on machine learning. PmLR, 2021, pp. 8748–8763.
- [4] J. Li, D. Li, S. Savarese, and S. Hoi, "Blip-2: Bootstrapping languageimage pre-training with frozen image encoders and large language models," in *International conference on machine learning*. PMLR, 2023, pp. 19730–19742.
- [5] L. H. K. Wong, X. Kang, K. Bai, and J. Zhang, "A survey of robotic navigation and manipulation with physics simulators in the era of embodied ai," arXiv preprint arXiv:2505.01458, 2025.
- [6] D. S. Chaplot, D. P. Gandhi, A. Gupta, and R. R. Salakhutdinov, "Object goal navigation using goal-oriented semantic exploration," *Advances in Neural Information Processing Systems*, vol. 33, pp. 4247–4258, 2020.
- [7] S. K. Ramakrishnan, D. S. Chaplot, Z. Al-Halah, J. Malik, and K. Grauman, "Poni: Potential functions for objectgoal navigation with interaction-free learning," in *Proceedings of the IEEE/CVF Conference* on Computer Vision and Pattern Recognition, 2022, pp. 18890–18900.
- [8] M. Khanna, R. Ramrakhya, G. Chhablani, S. Yenamandra, T. Gervet, M. Chang, Z. Kira, D. S. Chaplot, D. Batra, and R. Mottaghi, "Goat-bench: A benchmark for multi-modal lifelong navigation," in Proceedings of the IEEE/CVF Conference on Computer Vision and Pattern Recognition, 2024, pp. 16373–16383.
- [9] M. Savva, A. Kadian, O. Maksymets, Y. Zhao, E. Wijmans, B. Jain, J. Straub, J. Liu, V. Koltun, J. Malik et al., "Habitat: A platform for embodied ai research," in *Proceedings of the IEEE/CVF international* conference on computer vision, 2019, pp. 9339–9347.
- [10] M. Chang, T. Gervet, M. Khanna, S. Yenamandra, D. Shah, S. Y. Min, K. Shah, C. Paxton, S. Gupta, D. Batra, R. Mottaghi, J. Malik, and D. S. Chaplot, "Goat: Go to any thing," 2023.
- [11] H. Luo, A. Yue, Z.-W. Hong, and P. Agrawal, "Stubborn: A strong baseline for indoor object navigation," in 2022 IEEE/RSJ International Conference on Intelligent Robots and Systems (IROS). IEEE, 2022, pp. 3287–3293.
- [12] R. Ramrakhya, E. Undersander, D. Batra, and A. Das, "Habitat-web: Learning embodied object-search strategies from human demonstrations at scale," in *Proceedings of the IEEE/CVF conference on computer vision and pattern recognition*, 2022, pp. 5173–5183.
- [13] K. Ehsani, T. Gupta, R. Hendrix, J. Salvador, L. Weihs, K.-H. Zeng, K. P. Singh, Y. Kim, W. Han, A. Herrasti et al., "Spoc: Imitating shortest paths in simulation enables effective navigation and manipulation in the real world," arXiv preprint arXiv:2312.02976, 2023.
- [14] T. Gervet, S. Chintala, D. Batra, J. Malik, and D. S. Chaplot, "Navigating to objects in the real world," *Science Robotics*, vol. 8, no. 79, p. eadf6991, 2023.
- [15] S. Y. Gadre, M. Wortsman, G. Ilharco, L. Schmidt, and S. Song, "Cows on pasture: Baselines and benchmarks for language-driven zero-shot object navigation," in *Proceedings of the IEEE/CVF Conference on Computer Vision and Pattern Recognition*, 2023, pp. 23 171–23 181.
- [16] N. Yokoyama, S. Ha, D. Batra, J. Wang, and B. Bucher, "Vlfm: Vision-language frontier maps for zero-shot semantic navigation," in 2024 IEEE International Conference on Robotics and Automation (ICRA). IEEE, 2024, pp. 42–48.
- [17] P. Wu, Y. Mu, B. Wu, Y. Hou, J. Ma, S. Zhang, and C. Liu, "Voronav: Voronoi-based zero-shot object navigation with large language model," arXiv preprint arXiv:2401.02695, 2024.
- [18] Y. Long, W. Cai, H. Wang, G. Zhan, and H. Dong, "Instructnav: Zero-shot system for generic instruction navigation in unexplored environment," arXiv preprint arXiv:2406.04882, 2024.

- [19] D. Batra, A. Gokaslan, A. Kembhavi, O. Maksymets, R. Mottaghi, M. Savva, A. Toshev, and E. Wijmans, "Objectnav revisited: On evaluation of embodied agents navigating to objects," arXiv preprint arXiv:2006.13171, 2020.
- [20] J. Krantz, S. Lee, J. Malik, D. Batra, and D. S. Chaplot, "Instance-specific image goal navigation: Training embodied agents to find object instances," arXiv preprint arXiv:2211.15876, 2022.
- [21] X. Sun, L. Liu, H. Zhi, R. Qiu, and J. Liang, "Prioritized semantic learning for zero-shot instance navigation," in *European Conference* on *Computer Vision*. Springer, 2024, pp. 161–178.
- [22] C. Huang, O. Mees, A. Zeng, and W. Burgard, "Visual language maps for robot navigation," in 2023 IEEE International Conference on Robotics and Automation (ICRA). IEEE, 2023, pp. 10608–10615.
- [23] M. Wortsman, K. Ehsani, M. Rastegari, A. Farhadi, and R. Mottaghi, "Learning to learn how to learn: Self-adaptive visual navigation using meta-learning," in *Proceedings of the IEEE/CVF conference on computer vision and pattern recognition*, 2019, pp. 6750–6759.
- [24] F. L. Busch, T. Homberger, J. Ortega-Peimbert, Q. Yang, and O. Andersson, "One map to find them all: Real-time open-vocabulary mapping for zero-shot multi-object navigation," arXiv preprint arXiv:2409.11764, 2024.
- [25] N. Kim, O. Kwon, H. Yoo, Y. Choi, J. Park, and S. Oh, "Topological semantic graph memory for image-goal navigation," in *Conference on Robot Learning*. PMLR, 2023, pp. 393–402.
- [26] H. Yin, X. Xu, L. Zhao, Z. Wang, J. Zhou, and J. Lu, "Unigoal: Towards universal zero-shot goal-oriented navigation," arXiv preprint arXiv:2503.10630, 2025.
- [27] X. Lei, M. Wang, W. Zhou, and H. Li, "Gaussnav: Gaussian splatting for visual navigation," *IEEE Transactions on Pattern Analysis and Machine Intelligence*, 2025.
- [28] B. Kerbl, G. Kopanas, T. Leimkühler, and G. Drettakis, "3d gaussian splatting for real-time radiance field rendering." ACM Trans. Graph., vol. 42, no. 4, pp. 139–1, 2023.
- 29] G. Chen and W. Wang, "A survey on 3d gaussian splatting," 2025.
- [30] H. Matsuki, R. Murai, P. H. Kelly, and A. J. Davison, "Gaussian splatting slam," in *Proceedings of the IEEE/CVF Conference on Computer Vision and Pattern Recognition*, 2024, pp. 18 039–18 048.
- [31] N. Keetha, J. Karhade, K. M. Jatavallabhula, G. Yang, S. Scherer, D. Ramanan, and J. Luiten, "Splatam: Splat track & map 3d gaussians for dense rgb-d slam," in *Proceedings of the IEEE/CVF Conference on Computer Vision and Pattern Recognition*, 2024, pp. 21 357–21 366.
- [32] M. Qin, W. Li, J. Zhou, H. Wang, and H. Pfister, "Langsplat: 3d language gaussian splatting," in *Proceedings of the IEEE/CVF Conference on Computer Vision and Pattern Recognition*, 2024, pp. 20051–20060.
- [33] S. Zhou, H. Chang, S. Jiang, Z. Fan, Z. Zhu, D. Xu, P. Chari, S. You, Z. Wang, and A. Kadambi, "Feature 3dgs: Supercharging 3d gaussian splatting to enable distilled feature fields," in *Proceedings of the IEEE/CVF Conference on Computer Vision and Pattern Recognition*, 2024, pp. 21676–21685.
- [34] J.-C. Shi, M. Wang, H.-B. Duan, and S.-H. Guan, "Language embedded 3d gaussians for open-vocabulary scene understanding," in Proceedings of the IEEE/CVF Conference on Computer Vision and Pattern Recognition, 2024, pp. 5333–5343.
- [35] Y. Wu, J. Meng, H. Li, C. Wu, Y. Shi, X. Cheng, C. Zhao, H. Feng, E. Ding, J. Wang et al., "Opengaussian: Towards point-level 3d gaussian-based open vocabulary understanding," arXiv preprint arXiv:2406.02058, 2024.
- [36] B. Yamauchi, "Frontier-based exploration using multiple robots," in Proceedings of the second international conference on Autonomous agents, 1998, pp. 47–53.
- [37] A. Kirillov, E. Mintun, N. Ravi, H. Mao, C. Rolland, L. Gustafson, T. Xiao, S. Whitehead, A. C. Berg, W.-Y. Lo et al., "Segment anything," in *Proceedings of the IEEE/CVF international conference* on computer vision, 2023, pp. 4015–4026.
- [38] J. A. Sethian, "A fast marching level set method for monotonically advancing fronts." proceedings of the National Academy of Sciences, vol. 93, no. 4, pp. 1591–1595, 1996.
- [39] X. Zou, J. Yang, H. Zhang, F. Li, L. Li, J. Wang, L. Wang, J. Gao, and Y. J. Lee, "Segment everything everywhere all at once," *Advances in neural information processing systems*, vol. 36, pp. 19769–19782, 2023.
- [40] P. Lindenberger, P.-E. Sarlin, and M. Pollefeys, "Lightglue: Local feature matching at light speed," in *Proceedings of the IEEE/CVF* international conference on computer vision, 2023, pp. 17 627–17 638.